Active media under rotational forcing

Vicente Pérez-Villar, Jose L. F. Porteiro,* and Alberto P. Muñuzuri
Group of Complex Systems, Faculty of Physics, University of Santiago de Compostela, E-15782 Santiago de Compostela, Spain
(Received 24 March 2006; published 3 October 2006)

The bubble-free Belousov-Zhabotinsky reaction has been used to study the effects of centrifugal forces on autowave propagation. The reaction parameters were chosen such that the system oscillates naturally creating target waves. In the present study, the system was forced to rotate with a constant velocity around a central axis. In studying the effects of such a forcing on the system, we focused on target dynamics. The system reacts to this forcing in different ways, the most spectacular being a dramatic increase in the period of the target, the effect growing stronger as we move away from the center of rotation. A numerical study was carried out using the two-variable Oregonator model, modified to include convective effects through the diffusion coefficient. The numerical results showed a good qualitative agreement with those of the experiments.

DOI: 10.1103/PhysRevE.74.046203 PACS number(s): 82.40.Ck, 47.70.Fw, 82.20.−w, 83.50.Xa

I. INTRODUCTION

The ability of active media to organize themselves into spiral waves, targets, and other spatiotemporal structures and their ability to interact with external force fields has been the object of numerous experimental and numerical studies. These active media can be observed in a variety of systems from galaxies to bacteria colonies such as the amoeba *Dictyostelium Discoideum* [1], in chemical systems such as the Belousov-Zhabotinsky reaction [3], in signal propagation in the nervous system [2], and in the cardiac tissue.

Active chemical systems are often used to simulate these structures. They arise in systems where only reaction-diffusion processes can take place [4,5] due to the propagation properties of the wave front. In order to understand the mixing processes that result from the interaction of external force fields with the system, it is necessary to develop a more general description of the problem including advection as well as reaction-diffusion processes [6], or to modify the diffusion coefficient to take into account the changes in the interactions between chemical species that result from the presence of electrical fields [7].

The influence of temperature and density gradients has been studied by several authors [8,9], as well as the effects of the flow generated by these gradients on the gravitational field [10]. In this paper, we will investigate the effect of centrifugal forces on a diffusion-reaction generated target in a two-dimensional active medium, such that no density gradient-induced flows exist.

II. EXPERIMENTAL RESULTS

The experimental setup consisted of a rotating platform that was driven by a DC electric motor; the speed of rotation was controlled by varying the motor supply voltage. The reaction took place in a closed unstirred reactor composed of two parallel circular and transparent plates separated by a fixed gap of 0.3 mm. As the liquid reaction did not present any free surface, the thickness of the reaction was kept constant for any rotational frequency. The inner diameter of the Petri dish containing the reactants was kept constant and equal to 10 cm for all experiments here reported.

For a typical experiment, after the reactants were placed in the reactor, the rotational speed was slowly increased to a set value and then held constant for a period during which observations were made and measurements were taken. The speed was slowly increased again to a higher value and the procedure repeated until data was obtained for all desired rotational speeds.

To visualize the reaction we used a CCD camera connected to a DVD recorder and a PC for post-processing. The 1,4-cyclohexanedione-(CHD) based, bubble-free BZ reaction was used with initial concentrations of $1.5M$ H_2SO_4, $0.1M$ CHD, $0.06M$ $NaBrO_3$, $0.02M$ NaBr, and $7.5\times10^{-4}M$ Ferroin. These parameters correspond with the oscillatory regime of the reaction. The temperature was kept at 20 ± 1 °C. No gel layer was considered to immobilize the catalyzer as it may destroy any effect in the system.

Figure 1 depicts the dynamics of a *target* at 12.5 mm from the center of rotation at 30 rpm (a), 50 rpm (b), and 70 rpm (c). Both (b) and (c) show an increase of their period with respect to (a). At 70 rpm (c), the increase is such that the target center disappears and the system shows a tendency towards excitability (that is, we could not measure the next oscillation before the target was destroyed by spiral waves at the boundaries). Note that an increase of the oscillation period of the target is translated into an increase of the wavelength as the front velocity remains constant. At larger distances from the center, target dynamics are influenced by the boundary and oscillation periods are altered.

In order to establish the influence of the distance from the center of rotation and different rotational speeds on the period, two targets were studied, one at 10.1 mm and another at 19.8 mm from the rotational center. The experimental results are shown, in normalized form, in Fig. 2. The two sets of data are here plotted and almost fit a straight line when the normalized period of oscillation (T/T_0) is plotted versus $\omega r/v_0$. The parameters used for normalizing are

*Permanent address: University of South Florida, USA.

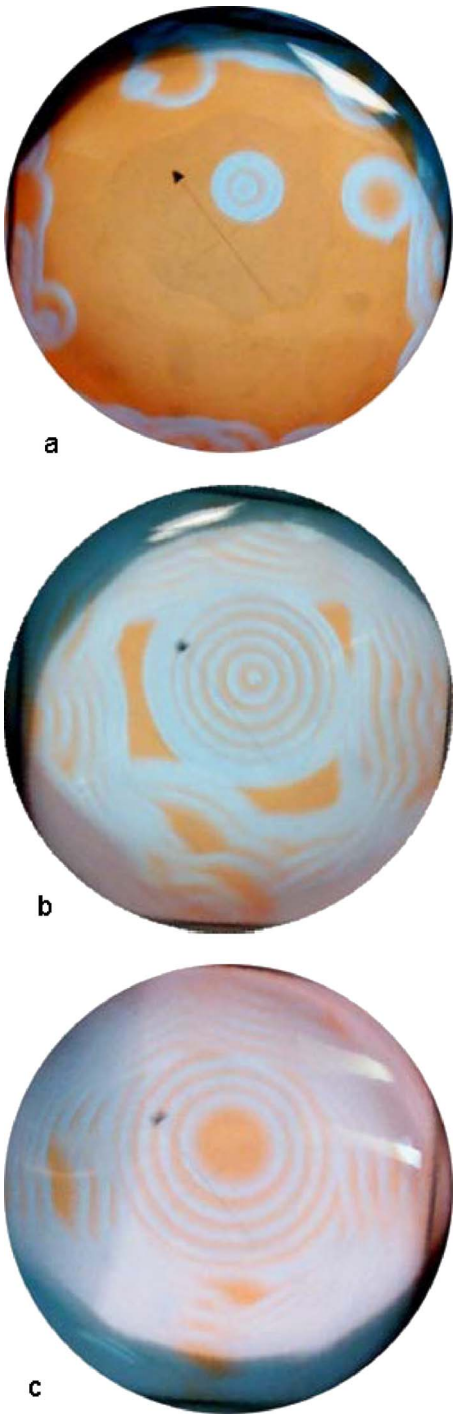

FIG. 1. (Color online) Behavior of a target located at 12.5 mm from the rotational center for different velocities of rotation (a) 30 rpm, (b) 50 rpm, and (c) 70 rpm. (The arrow in the figures is just a reference that shows the orientation of the Petri dish.)

the period of oscillation without rotation, $T_0=22$ s, and the velocity of a wave front in the absence of rotation, $v_0=0.11$ mm/s. Note that the period of oscillation increases with both the rotation frequency ω and the distance to the rotation center r. The dependence is clearly linear (at least for the parameter range analyzed) with a least-square linear fit given by $T/T_0=p_1(wr/v_0)+p_2$ with

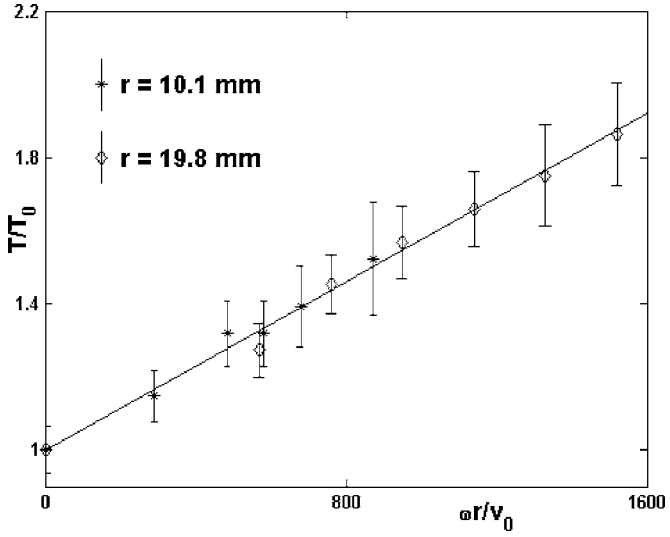

FIG. 2. Oscillation periods (measured at the center of each target) vs the velocity of rotation times the distance from the target center to the rotation center normalized by the wave-front velocity without rotational forces. The experimental data is normalized by $T_0=22$ s and $v_0=0.11$ mm/s. Two sets of data are plotted in the same figure corresponding to two different distances from the rotational center, 10.1 mm and 19.8 mm.

$p_1=0.0006\pm0.0001$, $p_2=0.99\pm0.04$, and a correlation coefficient of 0.996.

III. NUMERICAL MODEL

The dynamics of a two-dimensional reaction-diffusion medium subject to a force field generated by a rotation around its center is given by

$$\frac{\partial \mathbf{q}}{\partial t} = \mathbf{Q}(\mathbf{q}, \boldsymbol{\mu}) - \boldsymbol{\nabla} \cdot \mathbf{J}, \tag{1}$$

where $\mathbf{q}$ is the species concentration vector, $\mathbf{Q}$ is a source term, $\mathbf{J}$ is a molecular diffusion flux-vector matrix associated with the rotation and $\boldsymbol{\mu}$ is a vector describing system characteristics.

Our experimental work was carried out using the Belousov-Zhabotinsky (BZ) reaction, which can be modeled by the two-variable (2V) Oregonator model. The two-dimensional velocity field resulting from the body rotation $\boldsymbol{\omega}$ around the Z axis is given by $\mathbf{V}=\mathbf{r}\wedge\boldsymbol{\omega}$, where $\mathbf{r}$ is the position vector of our solution element with respect to the center of rotation.

The resulting Oregonator 2V equations are then

$$\frac{\partial u}{\partial t} = \frac{1}{\epsilon}\left(u(1-u) - fv\frac{q-u}{q+u}\right) - \boldsymbol{\nabla}\cdot\mathbf{J}_u,$$

$$\frac{\partial v}{\partial t} = u - v - \boldsymbol{\nabla}\cdot\mathbf{J}_v, \tag{2}$$

where (u,v) are the state variables representing the ($HBrO_2$) and (Ferroin) concentrations, and f, q, and ϵ are constants related to reaction kinetics [11]. Tyson's "Lo" kinetic values

[12] were used when scaling Eq. (1) using $\delta = 1/0.018$ s.u./cm and $\tau = 1/21$ t.u./s [8] as length and time scaling factors (s.u. stands for space units and t.u. stands for time units).

The values of f, q, and ϵ were chosen so that our numerical model would reproduce the oscillating regime exhibited by our experiments. A linear stability analysis of Eq. (2) allows the use of $f=1.4$, $q=0.002$, and $\epsilon=0.2$ as the most appropriate values for our simulations, and they were used throughout all numerical work. Vectors $\mathbf{J}_u$ and $\mathbf{J}_v$ are the scaled fluxes of components u and v.

We have considered that, due to the rotation, the chemical components will be subject to centrifugal and Coriolis forces as given by $\mathbf{F}=\omega^2\mathbf{r}+2\mathbf{V}\wedge\boldsymbol{\omega}$. These forces will act upon the components modifying their fluxes [13]. A linear approximation of the interaction of fluxes and forces was developed and the obtained fluxes were

$$\mathbf{J}_i = 3\omega^2\mathbf{r}D_i\frac{M_i\rho_i}{RT}(1-\rho v_i) - D_i\nabla\rho_i. \tag{3}$$

The first term represents the contribution of the rotational forces, and the second that of molecular diffusion. Here we have used $\mathbf{J}_i$, D_i, M_i, ρ_i, and v_i, to represent the flux, molecular diffusion coefficient, molecular mass, density, and specific volume of components u and v (represented by index i) in a solution of density ρ at a temperature T subject to a rotation ω. R is the ideal gas constant (that naturally appears when using the expression for the chemical potential $\mu=\mu_0+RT\ln\rho$). In obtaining this equation we have assumed an ideal solution behavior ($\rho\approx 1g/cc$).

Using again Tyson's "Lo" kinetic values [12] to scale the fluxes we obtain

$$\mathbf{J}_u = B_u u\mathbf{r} - D_u\nabla u, \quad \mathbf{J}_v = B_v v\mathbf{r} - D_v\nabla v. \tag{4}$$

We can now write the corresponding Oregonator 2V equations that describe the reaction dynamics for a system under rotational forces;

$$\frac{\partial u}{\partial t} = \frac{1}{\epsilon}\left(u(1-u) - fv\frac{q-u}{q+u}\right) - B_u\nabla(u\mathbf{r}) + D_u\Delta u,$$

$$\frac{\partial v}{\partial t} = u - v - B_v\nabla(v\mathbf{r}) + D_v\Delta v, \tag{5}$$

where D_u and D_v are dimensionless diffusion coefficients of ($HBrO_2$) and (Ferroin), respectively, and B_u and B_v are dimensionless parameters associated with the rotation of the solution

$$B_u = \omega^2 A(1-\rho v_u)D_u, \quad B_v = \omega^2 A(1-\rho v_v)D_v\frac{M_v}{M_u}. \tag{6}$$

Here $A=(3M_u\tau^2)/(RT\delta^2)$, is a dimensionless constant, M_u and M_v are the molecular masses of ($HBrO_2$) and (Ferroin), and ω the dimensionless rotational speed.

To the best of our knowledge, there are no reliable experimental values for the specific volumes [9,10,12,14], appearing in Eq. (6). In order to reproduce accurately the dynamics of the Belousov-Zhabotinsky reaction with a 2V Oregonator model, we make in Eq. (6),

$$A(1-\rho v_u) = A(1-\rho v_v) = K. \tag{7}$$

In this way, the parameters associated with the rotation become

$$B_u = K\omega^2 D_u, \quad B_v = K\omega^2 D_v\frac{M_v}{M_u}. \tag{8}$$

The set of equations [Eqs. (5)] was integrated using the Alternating Direct Implicit (ADI) [16] method with mesh sizes (in all cases) of 257×257 (pixel^2), step sizes $\Delta x=\Delta y=0.78125$ s.u. and a time step of $\Delta t=0.0001$ t.u. Zero-flux conditions were set for all chemical concentrations at the domain boundaries. A fully developed target with a period of oscillation $T_0=7.103$ t.u was used as the initial state for our simulations. The diffusion coefficients D_u and D_v were chosen as 1 and 0.6, respectively, [10]. $K=-2.5\times10^{-5}$ in all simulations here presented.

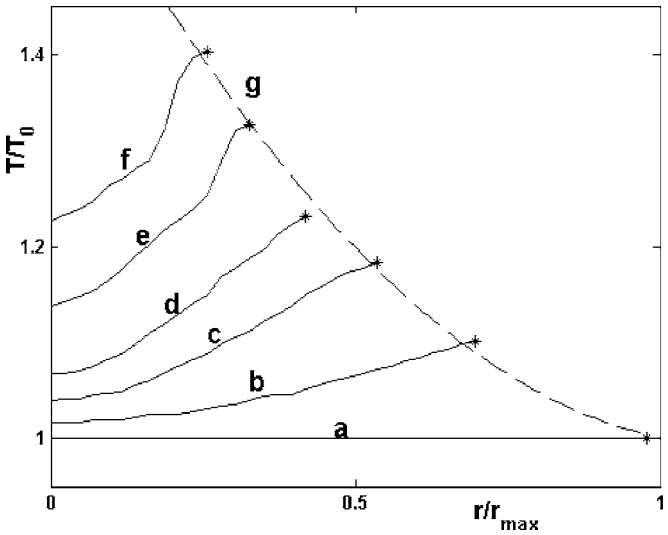

FIG. 3. Normalized period of oscillation vs normalized distance to the rotational center for values of $K\omega^2$ of (a) 0, (b) −0.0037, (c) −0.0074, (d) −0.011, (e) −0.0184, and (f) −0.0257. As the rotation speed and/or the distance increase, border effects become more pronounced and there is a boundary, (g) in the figure, beyond which they cannot be ignored.

IV. NUMERICAL RESULTS

Rotational speed influences reaction dynamics through the term $K\omega^2$ as indicated by Eq. (8). The influence of $K\omega^2$ on the period of a target located at different distances from the center of rotation is shown in Fig. 3. The oscillation period has been normalized with $T_0=7.103$ t.u. corresponding to the oscillation period in the absence of rotation. The maximum distance from the center of rotation, $r_{max}=100.9$ s.u., was used to normalize distances. The normalized periods of oscillation are shown as a function of the normalized distance for values of $K\omega^2$ of (a) 0, (b) −0.0037, (c) −0.0074, (d) −0.011, (e) −0.0184, and (f) −0.0257. The period of oscillation is observed to increase with both distance and the

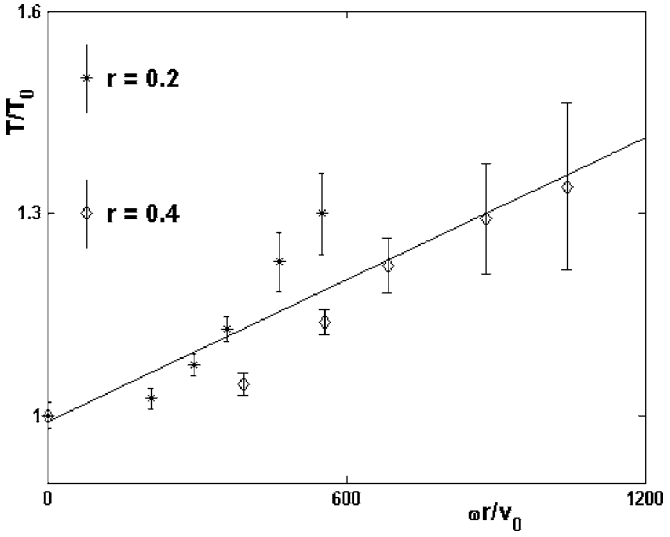

FIG. 4. Normalized period of oscillation vs the velocity of rotation times the distance from the target center to the rotation center normalized by the wave-front velocity without rotational forces. The data are normalized by T_0=7.1 t.u. and v_0=2.7 s.u./t.u. Two sets of data are plotted in the same figure corresponding to two different normalized distances from the rotational center, 0.2 s.u. and 0.4 s.u.

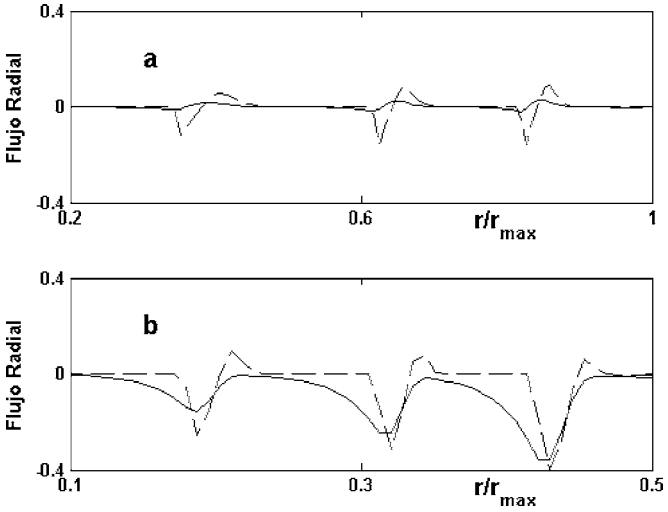

FIG. 5. Radial components of the fluxes for u (dashed line) and v (solid line). Two cases are plotted for (a) $K\omega^2=0$ and (b) $K\omega^2=-0.011$.

speed of rotation. As the rotation speed and/or distance increase, border effects become more pronounced and there is a boundary, (g) in the figure, beyond which they cannot be ignored.

Figure 4 plots the normalized periods of oscillation versus $\omega r/v_0$ for two sets of numerical data corresponding to normalized distances of 0.2 and 0.4, respectively (parameters used for normalizing T_0=7.1 t.u. and v_0=2.7 s.u./t.u.). It is important to note that here, as in the experimental case shown in Fig. 2, the dependence is qualitatively linear. A least-square linear fit gives $p_1=0.0004\pm0.0001$, $p_2=0.99\pm0.03$, and a correlation coefficient of 0.91 [being $T/T_0=p_1(wr/v_0)+p_2$]. Also note that the slopes of the experimental and numerical curves are compatible within the experimental errors.

From Eq. (4) the radial components of the fluxes can be obtained

$$\mathbf{R}_u = \left(B_u u|\mathbf{r}| - D_u \frac{\partial u}{\partial|\mathbf{r}|}\right)\mathbf{e}_r,$$

$$\mathbf{R}_v = \left(B_v v|\mathbf{r}| - D_v \frac{\partial v}{\partial|\mathbf{r}|}\right)\mathbf{e}_r, \quad (9)$$

where $\mathbf{e}_r$ is the radial unitary vector.

The period increase resulting from the rotation can be attributed to an increase of the radial fluxes. Figure 5 shows the radials fluxes, as described by Eq. (9), as a function of the radial distance for several propagation fronts. Radial fluxes for $K\omega^2=0$ (a) are smaller, in absolute value, than those obtained with $K\omega^2=-0.011$ (b), which can also be observed to increase with the distance from the center of rotation. Also note that the inhibitor (Ferroin) flux in (b) is larger than the activator flux ($HBrO_2$), thus, the appearance of a new front wave is slowed down and the periods increased. In case (a), with no centrifugal forces, the situation is just the opposite, the inhibitor flux is smaller than the activator flux, thus the generation of a new front wave is not inhibited. As the distance to the rotational center is increased, the inhibitor flux may become large enough as to completely suppress the appearance of a new front, so that this particular region may become excitable. Note that the global effect of the rotation of the system is translated into an increase of the effective diffusion coefficient of the chemicals; there is no flow in the system once the stationary regime is achieved. It is the increase of the effective diffusion coefficients that causes larger radial fluxes and, thus, increases the period of oscillation. Also note that although the effective diffusion coefficients are increased, there is no transport of chemicals and, thus, no flow in the system.

V. CONCLUSIONS

Both our numerical and experimental results indicate that the centrifugal forces resulting from a rotation, when acting on a target generated on an active oscillating medium, increase its oscillation period and that this increase becomes larger as we move away from the center of rotation. The numerical simulations qualitatively describe the experimental results, indicating that the increase in period is due to a centrifugal-force-induced increase in inhibitor dispersion that delays the appearance of the activator. The effect becomes more pronounced as we move away from the center of rotation. In the limit, the medium loses its oscillating character and we can consider its oscillating period to be infinite. Such a behavior is shown in Fig. 1(c) and can be directly attributed to a loss in the oscillating nature of the solution as a consequence of inhibitor dispersion. Similarly, this interpretation could justify the appearance of cardiac function disruptions on individuals subject to extreme centrifugal force exposure [15].

ACKNOWLEDGMENTS

This work has been supported by the MCyT (Spain) under project No. FIS2004-03006 and Xunta de Galicia (Spain) under project No. PGIDIT05PXIC20607PN. We would like to thank Dr. V. Pérez-Muñuzuri for useful comments. All numerical computations were performed at the Centro de Supercomputación de Galicia (Spain).

[1] http://www.zi.biologie.uni-muenchen.de/zoologie/dicty/dicty.html

[2] A. M. Turing, Philos. Trans. R. Soc. London, Ser. B **237**, 37 (1952); J. D. Murray, *Mathematical Biology* (Springer-Verlag, Berlin, 1989); M. H. Cohen and A. Robertson, J. Theor. Biol. **31**, 119 (1971); P. N. Devreotes, M. J. Potel, and S. A. MacKay, Dev. Biol. **96**, 405 (1983).

[3] A. N. Zaikin and A. M. Zhabotinsky, Nature (London) **255**, 535 (1970); A. T. Winfree, Science **175**, 634 (1972); *Chemical Waves and Patterns*, edited by R. Kapral and K. Showalter (Kluwer, Dordrecht, 1995); S. K. Scott, *Chemical Chaos* (Oxford University Press, New York, 1991).

[4] V. Pérez-Muñuzuri, R. Aliev, B. Vasiev, and V. Pérez-Villar, and V. I. Krinsky, Nature (London) **353**, 740 (1991); V. Pérez-Muñuzuri, R. Aliev, B. Vasiev, and V. I. Krinsky, Physica D **56**, 229 (1992); O. Steinbock, V. S. Zykov, and S. C. Müller, Nature (London) **366**, 322 (1993); A. P. Muñuzuri, M. Gómez-Gesteira, V. Pérez-Muñuzuri, V. I. Krinsky, and V. Pérez-Villar, Phys. Rev. E **50**, 4258 (1994).

[5] I. Sendiña-Nadal, S. Alonso, V. Pérez-Muñuzuri, M. Gómez-Gesteira, V. Pérez-Villar, L. Ramírez-Piscina, J. Casademunt, J. M. Sancho, and F. Sagués, Phys. Rev. Lett. **84**, 2734 (2000); V. Pérez-Muñuzuri, F. Sagués, and J. M. Sancho, Phys. Rev. E **62**, 94 (2000).

[6] M. S. Paoletti and T. H. Solomon, Phys. Rev. E **72**, 046204 (2005); Changsong Zhou, Jürgen Kurths, Zoltán Neufeld, and István Z. Kiss, Phys. Rev. Lett. **91**, 150601 (2003); Zoltán Neufeld, István Z. Kiss, Changsong Zhou, and Jürgen Kurths, *ibid.* **91**, 084101 (2003); Zoltán Neufeld, *ibid.* **87**, 108301 (2001).

[7] J. L. F. Porteiro, V. Pérez-Muñuzuri, A. P. Muñuzuri, and V. Pérez-Villar, Physica D **69**, 309 (1993).

[8] D. A. Vásquez, B. F. Edwards, and J. M. Wilder, Phys. Rev. A **43**, 6694 (1991); D. A. Vázquez, J. W. Wilder, and B. F. Edwards, Phys. Fluids A **4**, 2410 (1992); D. A. Vázquez, J. W. Wilder, and B. F. Edwards, J. Chem. Phys. **98**, 2138 (1993); J. W. Wilder, D. A. Vásquez, and B. F. Edwards, Phys. Rev. E **47**, 3761 (1993); D. A. Vásquez, J. M. Littley, J. W. Wilder, and B. F. Edwards, *ibid.* **50**, 280 (1994); Y. Wu, D. A. Vásquez, B. F. Edwards, and J. W. Wilder, *ibid.* **51**, 1119 (1995); D. A. Vásquez and C. Lengacher, *ibid.* **58**, 6865 (1998).

[9] J. A. Pojman and I. R. Epstein, J. Phys. Chem. **94**, 4966 (1990); J. A. Pojman, I. R. Epstein, and T. McManus, *ibid.* **95**, 1299 (1991); J. A. Pojman, I. R. Epstein, and I. Nagy, *ibid.* **95**, 1306 (1991); J. A. Pojman, R. Craven, A. Jhan, and W. West, *ibid.* **96**, 7476 (1992); I. P. Nagy and J. A. Pojman, *ibid.* **97**, 3443 (1993).

[10] V. Pérez-Villar, A. P. Muñuzuri, and V. Pérez-Muñuzuri, Phys. Rev. E **61**, 3771 (2000); V. Pérez-Villar, A. P. Muñuzuri, M. N. Lorenzo, and V. Pérez-Muñuzuri, *ibid.* **66**, 036309 (2002); J. I. Ramos, Chaos, Solitons Fractals **12**, 1897 (2001); **12**, 2267 (2001).

[11] J. Tyson and P. C. Fife, J. Chem. Phys. **73**, 2224 (1980).

[12] J. J. Tyson, in *Oscillations and Traveling Waves in Chemical Systems*, edited by R. J. Field and M. Burger (Wiley-Interscience, New York, 1985).

[13] S. R. de Groot and P. Mazur, *Non-Equilibrium Thermodinamics* (North-Holland, Amsterdam, London, 1969).

[14] J. D. Dockery, J. P. Keener, and J. J. Tyson, Physica D **30**, 177 (1988).

[15] J. E. Whinnery, Aviat., Space Environ. Med. **61**, 716 (1990); I. McKenzie and K. K. Gillingham, *ibid.* **64**, 687 (1993).

[16] W. H. Press, S. A. Teukolsky, W. T. Vetterling, and B. P. Flannery, *Numerical Recipes in C*, 2nd ed. (Cambridge University Press, 1992).